Julie C. Fleischer
BioMechanical Engineering,
Delft University of Technology,
Delft 2628CD, The Netherlands
e-mail: j.c.fleischer@tudelft.nl

Jan C. Diehl
Associate Professor
Design for Sustainability,
Delft University of Technology,
e-mail: j.c.diehl@tudelft.nl

Linda S. G. L. Wauben
Professor
Healthcare Technology,
Rotterdam University of Applied Sciences,
Rotterdam 3015 GG, The Netherlands;
BioMechanical Engineering,
Delft University of Technology,
Delft 2628CD, The Netherlands
e-mail: l.s.g.l.wauben@hr.nl

Jenny Dankelman
Professor,
BioMechanical Engineering,
Delft University of Technology,
Delft 2628CD, The Netherlands
e-mail: j.dankelman@tudelft.nl

The Effect of Chemical Cleaning on Mechanical Properties of Three-Dimensional Printed Polylactic Acid

Three-dimensional (3D) printing may be a solution to shortages of equipment and spare parts in the healthcare sector of low- and middle-income countries (LMICs). Polylactic acid (PLA) for 3D printing is widely available and biocompatible, but there is a gap in knowledge concerning its compatibility with chemical disinfectants. In this study, 3D-printed PLA tensile samples were created with six different printer settings. Each of these six batches consisted of five sets with five or six samples. The first set remained untreated, the others were soaked in Cidex OPA or in a chlorine solution. These were applied for seven consecutive days or in 25 short cycles. All samples were weighed before and after treatment and subjected to a tensile test. Results showed that a third of the treatments led to an increase of the median weight with a maximum of 8.3%, however, the samples with the best surface quality did not change. The median strength increase was 12.5% and the largest decrease was 8.8%. The median stiffness decreased 3.6% in one set and increased in three others up to 13.6%. When 3D printing PLA medical tools, surface porosity must be minimized to prevent transfer of disinfectants to people. The wide variability of mechanical properties due to 3D printing itself and as a consequence of disinfection must be considered when designing medical tools by selecting appropriate printer settings. If these conditions are met, reusing 3D-printed PLA medical tools seems safe from a mechanical point of view. [DOI: 10.1115/1.4046120]

1 Introduction

Shortages of (functional) medical equipment are a well-known problem in low- and middle-income countries (LMICs), limiting the quality of available healthcare [1–3]. For example, in Kenya, healthcare facilities stock an average of 77% of the equipment recommended by the World Health Organization for their level of care, ranging from over 90% in high-level institutions to only 23% in a rural dispensary [1]. There are various possible causes for equipment shortage, including a complex and expensive procurement process, high maintenance costs, the need for consumables, the lack of context-fit, the unavailability of spare parts, and the limited local capacity to repair [2–5].

It has been suggested that three-dimensional (3D)-printed medical tools could reduce the equipment shortage and solve repair problems [6–10]. A large variety of designs have been proposed, including knobs for controlling microscopes, a low-cost videolaryngoscope, a stethoscope, umbilical cord clamps, and surgical instruments [6,8,9,11–13]. For example, Bhatia et al. proposed a high-utility surgical toolkit that includes various types of commonly used forceps, clamps, and a retractor, based on devices previously described in the literature [6]. They suggest polylactic acid (PLA) as a material for these 3D-printed surgical tools since it is biocompatible and widely available. Moreover, because of the low production price, it has been suggested that these instruments can be discarded after a single use [7]. However, in LMICs, disposable devices are often cleaned or sterilized and re-used [14]. Tools that are designed for reuse are better suited to the context in low-resource settings, and therefore, cleaning and sterilization of PLA must be taken into account [15,16].

Polylactic acid can be sterilized using dry heat and the material is compatible with ethylene oxide, gamma radiation, and electron beams. However, none of these methods are widely available in LMIC healthcare institutions [17]. Although autoclaves are present more often, the low glass transition temperature of PLA makes steam sterilization at $120 - 130\ ^{\circ}C$ unfeasible [17,18]. Therefore, PLA tools in LMICs are likely to be cleaned and sterilized using chemical cleaning agents such as Cidex OPA and chlorine solutions [19].

Knowledge about the effects of these chemical cleaning agents on the mechanical properties of 3D-printed medical tools is limited. PLA is not listed as Cidex OPA compatible, and to the best of our knowledge, there are no studies on cleaning PLA with medical disinfectants apart from the work of Rankin et al. [7,20]. They printed six surgical retractors and studied the forces that led to visual deformation and eventually to breaking of five of them. They soaked the sixth retractor in glutaraldehyde for 25 min and concluded that there was no difference in force required for deformation and breaking. However, surgical tools must be sterilized repeatedly and may be soaked in chemical cleaning agents for longer periods of time. Yew et al. found that PLA immersed in water absorbs up to 1% moisture, leading to a 6% loss of tensile strength for the wet samples and 16% reduction in elongation at break when the samples were still wet [21]. Drying of the samples at $80\ ^{\circ}C$ in a vacuum resulted in a 33% loss of tensile strength and reduction in the elongation at break by 47% compared to the control samples. A similar effect due to immersion in chemical cleaning agents might jeopardize safe use of PLA medical tools, specifically for 3D-printed PLA tools which tend to have porous surfaces [22].

When 3D printing, there is a wide choice of slicer settings that influence the quality of the printed product. Previous studies have shown that surface roughness, strength, stiffness, dimensional accuracy, and build time depend—among others—on layer thickness, print temperature, infill percentage, the number of shell perimeters, and print speed [23–27]. The perfect combination of settings depends on the desired properties of a product and is expected to vary for the wide range of medical tools that could be 3D printed. For example, Bhatia et al. state that infill densities between 60% and 80% provide the best combination of mechanics and flexibility for the instruments in their surgical toolkit [6].

Manuscript received August 15, 2019; final manuscript received January 15, 2020; published online February 11, 2020. Assoc. Editor: Boris Rubinsky.

A better understanding of the effects of commonly used chemical cleaning agents on various qualities of 3D-printed PLA is required to assess the suitability of this material for reusable medical devices. Therefore, the main objective of this study was to examine the changes in material stiffness, strength, and weight of 3D-printed PLA samples as a consequence of both long and short treatments with Cidex OPA and a chlorine solution. A subobjective was to identify the effect of the slicer settings on the stress–strain curves of the untreated samples.

2 Method

2.1 Sample Creation. Six batches (A–F) of tensile samples with different print qualities were created, allowing for assessment of the compatibility of these settings with chemical cleaning. Two Ultimaker 3 printers (Ultimaker, Geldermalsen, The Netherlands) were used to create the samples with white Ultimaker PLA and Table 1 lists the slicing settings in Cura 4.0 (Ultimaker, Geldermalsen, The Netherlands) for each batch. A batch consists of 25 or 30 samples, which were divided into 5 sets of 5 or 6 samples. For reading clarity, sets are denoted as a combination of a number and letter. For example, set 3 of batch D is denoted as D3. Each set underwent a different treatment as described in Sec. 2.2. The sample design matched the specifications listed in the ASTM D638 standard and was modeled to be 3 mm thick and 165 mm long [28].

Samples A–E were stacked on top of a flat surface with linear support between each layer and between the bottom layer and the print bed. Figure 1(*a*) shows the configuration used to print one batch and how this is split into 5 sets, each consisting of a vertical stack of samples. Sample F was all printed on the print bed in order to have the best possible surface quality. For batches C–F, a gyroid fill pattern was selected because it is the most isotropic pattern currently available in Cura as shown in Fig. 1(*b*). The print bed was always heated to 60 °C. Samples were removed from the print bed after they had cooled down to room temperature and support was manually removed, using a knife when required. Each sample was weighed twice using a Scaltec SBC 33 scale (Scaltech, Dubai, United Arab Emirates).

2.2 Cleaning Procedure

For each batch, the cleaning procedure was as follows:

- Set 1 was left untreated to serve as control group.
- Set 2 was placed in a transparent polypropylene container and soaked in approximately 0.5 L of Cidex OPA (Johnson & Johnson, New Brunswick, NJ) for 7 days. After removal from the containers, samples were rinsed three times with tap water and dried using cloth towels and weighed using the Scaltech SBC 33 scale.
- Set 3 was treated as set 2, but the samples were now soaked in a chlorine solution of 1000 ppm (2 Medicarine tablets (Ecolab, St. Paul, MN), dissolved in 3l tap water) for 7 days.
- Set 4 underwent 25 cycles of 15 min Cidex OPA soaks as per the instructions in the manual [20]. After each soak, the samples were rinsed three times with tap water and dried using cloth towels. Samples were weighed using a Kern Emb-602 (Kern & Sohn Gmbh, Balingen-Frommern, Germany) scale after the 25th cycle.
- Set 5 underwent 25 cycles of 10 min chlorine soaks in a transparent polypropylene container in accordance with the duration recommended by the World Health Organization [29]. Samples were weighed using a Kern Emb-602 scale-after the 25th cycle.

2.3 Tensile Tests. Tensile tests were performed according to the ASTM D368 standard using a Zwick & Roell (Ulm, Germany) 10 kN stage, a Zwick& Roell clip-on extensometer, and dedicated software TestXpert II [28]. No pretension was applied and samples were deformed at a rate of 5 mm/min until they broke. The gage thickness was kept constant at 3.5 mm for batches A–E. Due to the stacked printing of batches A–E, the bottom surfaces were very rough, and therefore, it was not possible to accurately measure the gage thickness. The gage width was measured at three places and averaged for samples of all batches. For batch F, the gage thickness was measured twice at the center of the sample and then averaged.

2.4 Data Processing. Data from the tensile tests were exported from TestXpert II and MATLAB R2018a (Mathworks, Natick, MA) was used for further processing. Toe-correction was executed as per the ASTM D638 standard [28]. For each sample, the stress and strain at break as well as the *E*-modulus were determined according to the ASTM D638 standard. Depending on the type of stress–strain curve, we also determined the stress and strain values at yield or 0.1% offset for each sample. All properties within a set were checked for normality using a one-sample Kolmogorov–Smirnov test and a two-sided Wilcoxon rank test was performed to determine whether the properties of the post-treatment batches differed significantly from the untreated ones. A *p*-value lower than 0.05 was considered significant.

The pretreatment weights of all sets within each batch were compared using the Wilcoxon rank test to determine the variability of the 3D printing process. Pre- and post-treatment weights from each set were also compared to estimate fluid absorption. In the remainder of this text, unless otherwise specified, values are provided as median (range).

2.5 Terminology. In stress–strain curves, the term *strength* is used to describe the point of highest stress, which can occur when the material yields or breaks. The yield and breaking point for two different stress–strain curves are indicated in Fig. 1(*c*). If a material has a yield stress, the term breaking *stress* is used to describe the stress at break and vice versa. Since both yield and breaking strength are observed within different batches in this study, the term stress will be used throughout the text to describe yield strength, yield stress, breaking strength, and breaking stress for readability.

Table 1 Printer settings used in Cura 4.0 for Ultimaker 3 printer

Batch	A Low quality	B High quality	C Medium fill	D Low fill	E Thin shell	F Bed
Layer height	0.25 mm	0.12 mm	0.12 mm	0.12 mm	0.12 mm	0.12 mm
Wall thickness	1.2 mm	1.2 mm	1.2 mm	1.2 mm	0.6 mm	1.2 mm
Top/bottom layers	2	4	4	4	2	4
Infill density	100%	100%	65%	30%	65%	65%
Infill pattern	Lines	Lines	Gyroid	Gyroid	Gyroid	Gyroid
Print temperature	205 °C	230 °C	230 °C	230 °C	230 °C	230 °C
Print speed	80 mm/s	50 mm/s	50 mm/s	50 mm/s	50 mm/s	50 mm/s
Brim	yes	yes	yes	yes	yes	yes
Support density	15%	15%	15%	15%	15%	0%
Stacking	yes	yes	yes	yes	yes	no
Number of samples per set	5	6	6	6	5	5

3 Results

A total of 165 samples were printed and tested. Due to incomplete recording of the measurement by the software, 3 samples in A4, 3 in C1, and 2 in C4 were removed, which represent 4.8% of the total number of printed samples. After sample removal, a total of 157 measurements were obtained. The medians and ranges of all sets for each mechanical property are also listed in Tables 4–8 in the Appendix.

3.1 Effects of Print Settings in Control Sets

3.1.1 Surface Quality and Mechanical Behavior. The support structure resulted in rough bottom surfaces for batches A–E as shown in Fig. 2. The print settings resulted in different types of mechanical behavior for the untreated sets as seen in Fig. 3(*a*). Each curve represents a sample from set 1 of a different batch. The selected curves have a yield stress that is closest to the average yield stress within their set, except for batch D for which a curve with average strain was selected. The stress–strain curves for batches A, B, and E are typical for ductile materials. Batches C and F are more brittle, and batch D shows a small region of plastic deformation. A clear yield point was only observed and determined for batch B.

3.1.2 Weight. The median and range of the weight of set 1 of each batch are presented in Table 2. The second row lists the pairs of sets within each batch that were significantly different after printing, ranging from 0 to 6 pairs. The range of weights was highest for the samples with a thin shell in batch E, although this was the only batch that did not have a print effect.

3.1.3 E-Modulus. The stiffness of the various untreated batches can be observed in the linear parts of Fig. 3(*a*) and are also reported as red diamonds in Fig. 3(*b*). Additionally, the numerical values are available in Table 4 in the Appendix. The high-quality printer settings for batch B yielded the stiffest material with an *E*-modulus of 2.8 (2.7–2.9) GPa, followed by batch F at 2.2 (2.2–2.3) GPa. The medium-fill batch C is slightly stiffer at 1.8 (1.8–1.8) GPa compared to the low quality batch A with a stiffness of 1.5 (1.5–1.7) GPa. Batches D and E had similar stiffness at 1.3 (1.3–1.4) GPa and 1.3 (1.0–1.4) GPa, respectively.

3.1.4 Strain and Stress at Yield. The red diamonds in Figs. 3(*c*) and 3(*d*) show the measured strains and stresses at 0.1% offset of the control samples of batches A and C–F. All numerical values are listed in the Appendix in Tables 5 and 6. For batch B, the values at the actual yield point are displayed and discussed. The median strain at yield at 0.1% offset ranged from 1.2 (1.2–1.3)% for batch C to 2.0 (1.9–2.3)% for batch B at the actual yield point. The widest range at 0.3% was observed in batch A with a strain at yield of 1.5 (1.3–1.6) %. The median stress at yield was highest at 46.0 (44.7–49.0) MPa for batch B and lowest for batch E at 17.4 (13.3–18.2) MPa at 0.1% offset.

3.1.5 Strain and Stress at Break. The red diamonds in Fig. 3(*e*) show the elongation at break for the control samples. All numerical values are listed in the Appendix in Tables 7 and 8. Batch A showed the highest rates of elongation at 8.2 (8.0–10.3)%, followed by batch B at 6.8 (3.7–8.3)%. The pattern for the stresses at break in Fig. 3(*f*) is similar to the stresses at yield, with the highest stress of 41.0 (39.8–43.0) for batch B. Batches D and E had very similar stresses of 20 (19.4–21.5) MPa and 20.5 (14.7–21.6) MPa, respectively.

3.2 Treatment Effect. Figure 3 includes the measured breaking stress, breaking strain, yield stress, yield strain, and *E*-modulus for all sets. All numerical values are also listed in Tables 3–8 in the Appendix.

3.2.1 Surface Quality and Mechanical Behavior. Some sets within batches A and D felt moist to the touch after drying and the cyclic treatments caused some samples to lose bits of material, visible as white specks and strands within the containers. Batch A was effectively turned into a brittle material after all treatments. Also, set B3 no longer showed a region of plastic deformation after 25 cycles in Cidex and also no longer had a clear yield point.

3.2.2 Weight. The bottom rows in Table 2 show the eight sets that showed a significantly different weight post-treatment, as well as the percentual change in their median weight. Except for batch B4 which showed a median decrease of 0.02%, all weights *increased*, indicating that the samples absorbed the liquid. The median and range for all sets pre- and post-treatment are listed in the Appendix in Table 3.

3.2.3 E-Modulus. The stiffness of most samples remained the same after treatment as seen in Fig. 3(*b*) and listed in Table 4. However, sets D5 ($p = 0.01$), F4 ($p = 0.01$), and F5 ($p = 0.01$) all showed a significant increase in stiffness after cyclic treatments with Cidex and chlorine. Using the values in Table 4, a maximum change of 13.6% in median stiffness was obtained for set F5. Increases in range were most notable in sets 2–4 in batch C and set A5. Set C5 showed a decrease of 3.6% in median stiffness at 1.7 (1.7–1.7) MPa ($p = 0.02$) compared to 1.8 (1.8–1.8) MPa in C1.

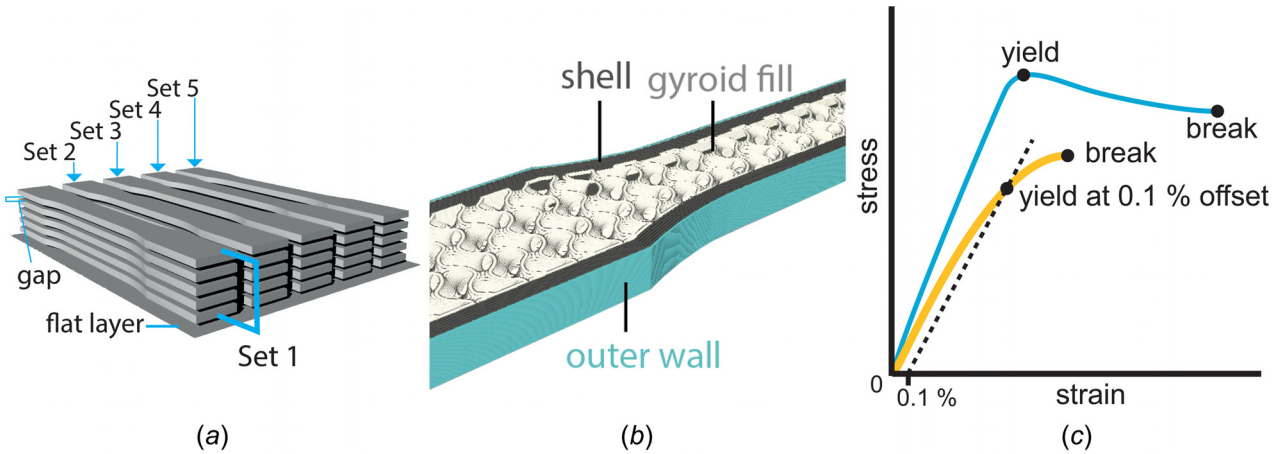

Fig. 1 Clarification of terminology used in 3D printing the samples and stress–strain curves: (*a*) Computer-aided design file of one batch illustrating how samples are stacked in the 3D printer and how sets are created and (*b*) preview from Cura, indicating the outer wall, shell, and gyroid fill structure of the samples. (*c*) Two types of stress–strain curves and the associated terminology. The thin solid curve represents a ductile material and the thicker solid curve represents a brittle material.

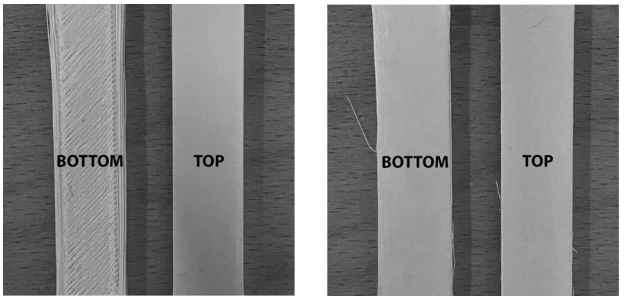

Fig. 2 Typical examples of surface quality. Left: example of a rough bottom and smooth top surface from batch B; right: example of smooth bottom and top surface from batch F.

3.2.4 Yield Characteristics. Figures 3(*c*) and 3(*d*) show the strain and stress at yield after different treatments. All numerical values are listed in the Appendix in Tables 5 and 6. Significant increases were found for sets C2 ($p = 0.01$), C3 ($p = 0.02$), C5 ($p = 0.01$), and D2 ($p = 0.03$), while an increase in range from 0.1% to 0.8% was observed for set C4 using the data in Table 5. The elongation significantly decreased for sets D4 ($p = 0.03$) and E4 ($p = 0.02$) after the cyclic treatments with Cidex.

The stress at 0.1% offset increased significantly for batches C2 ($p < 0.01$), C3 ($p = 0.02$), C5 ($p = 0.04$), D2 ($p = 0.04$), and D3 ($p < 0.01$). However, a decrease of 8.8% in median stress was seen for batch D4 after the cyclic Cidex treatment ($p = 0.01$). Using the data from Table 6, the largest increase in median yield stress was 12.5% for batch C2.

3.2.5 Breaking Characteristics. The break stress and strain are shown in Figs. 3(*e*) and 3(*f*). All numerical values are listed in the Appendix in Tables 7 and 8. The elongation at break after treatment was much shorter for all sets in batch A with $p = 0.01$ for sets A2, A3, and A5 and $p = 0.02$ for set A3. Elongation also decreased for set B3 ($p < 0.01$). Increased breaking stress was observed for A3 ($p = 0.03$), B3 ($p < 0.01$), D2 ($p = 0.01$), D3 ($p = 0.01$), and D5 ($p < 0.01$). However, breaking stress decreased for sets B4 ($p = 0.04$) and D4 ($p < 0.01$).

4 Discussion

In this study, six types of 3D-printed tensile samples were soaked in Cidex OPA or in a chlorine solution. Each solution was applied for seven consecutive days or in 25 short cycles with rinses in between. Eight sets increased in weight during treatment, with the median increase ranging from 0.3% to 8.3%. Three sets showed increased stiffness after the cyclic treatments and one showed decreased stiffness, the maximum change of the median stiffness was 13.6%. Both increases and decreases of stress and strain were found for the yield and breaking points, with a maximum increase of 12.5% and a maximum decrease of 8.8% or the median yield stress.

4.1 Effects of Print Settings. The mechanical properties of the untreated samples were similar to the results obtained in other studies that used comparable slicing parameters [26,30]. Akhoundi et al. (2010) created PLA samples with the same fill pattern and percentage at 40 mm/s on an unknown printer and measured a tensile strength of 54 MPa and stiffness of 3.4 GPa [30]. This is comparable to our findings of batch B, which had a strength of 46.0 (44.7–49.0) MPa and a stiffness of 2.8 (2.7–2.9) GPa. Furthermore, Pei et al. (2015) printed with 0.1 mm layer height on a RepRap printer and obtained a comparable tensile strength of 49.3 MPa.

The large decrease in strength of batch A compared to batch B is in line with expectations. A combination of a low temperature and high print speed is known to reduce stiffness and strength [24]. Reducing the fill percentage from 100% in batch B to 65% in batch C resulted in the same decrease of strength, using less material than in batch A. Using the same slicer settings, but printing the samples directly on the bed provided about 50% extra strength in batch F compared to batch C. The effect of printing partially supported surfaces is therefore very important to take into account when designing for 3D printing and printing directly on the print bed should be regarded as an effective way to maximize strength. A further reduction of infill led to decreased stiffness as expected in batch D. Reducing the number of shell perimeters to 2 in batch E led to a yield strength of 1.2 (1.2–1.3) MPa compared to 1.4 (1.4–1.5) MPa with 4 shell perimeters in batch C. This is comparable to findings by Pei et al. (2015), who found a 13% decrease for the same change in shell perimeters [26].

Although the findings discussed above provide insight about different mechanical properties of the untreated sets, no statistical comparison was done for these sets. In order to execute meaningful statistical tests, the study design should be adapted. The printer settings and samples that are compared should be carefully selected to identify relevant effects, and a correction should be applied to compensate for errors related to multiple comparisons. Also, all samples should be created on the same printer. Therefore, the value of the comparison of the untreated samples in this study lies in the fact that we observe different types of mechanical behavior which could form the starting point for designers looking for specific material properties.

The variability in weight between sets (listed in Tables 2 and 3) indicates that 3D printing results in differences between parts and this must be taken into account when designing printed parts.

4.2 Treatment Effect. For low quality prints in batch A, both long and short chemical cleaning with a chlorine solution or Cidex OPA led to a strong decrease in break strain, effectively changing the PLA from a ductile to a brittle material. The same effect was observed in the high quality set B3 after 25 cycles in Cidex.

4.2.1 Weight. Eight sets showed significant weight increase, despite the fact that strands and specks of material broke off the samples during the treatments, as seen in Table 2. Most percentual increases are comparable to the findings by Yew et al. who found a 1% increase, however, batch E showed much larger weight gain after the cyclic treatments of 8.3% in F4 and 6.6% in E5. This could be a result of fluid absorption into the material, but also the presence of fluid within the cavities of the gyroid fill. It seemed logical that the long-term treatments would also lead to significant weight gain, but this was not the case for batch E. It might be possible that fluid absorption and/or filling of material cavities is increased due to the water rinsing rather than soaking in the cleaning agent. The protocols used in this study did not allow for separate identification of weight gain through rinsing or soaking, hence this requires further experiments.

The high surface quality obtained by printing directly on the bed in batch F is likely responsible for protecting the sample from absorbing liquid, preventing weight gain within this batch. However, no general trend or explanation is found for the increased weight gain as a consequence of the printer settings for the other batches.

Sets in both batches A and E were moist to the touch, even after the drying period. Combined with the measured weight increase, there is clearly a chance that small amounts of Cidex OPA or chlorine solution can be transferred to tissues in contact with 3D-printed tools of low print quality or with thin shells and partial fill.

4.2.2 Tensile Strength and Stiffness. Spending seven days in the chemical cleaning agent increased the yield strength at 0.1% offset for the samples in sets C2, C3, D2, and D3. The cyclic chlorine treatments also increased the yield stress at 0.1% offset for set C5. However, the cyclic Cidex treatment decreased the yield stress at 0.1% offset for set D4. The maximum increase of the median was 2.5 MPa and the decrease was 1.6 MPa, around 10% of the original sample strengths. The maximum change in stiffness was 13.6% compared to the control samples.

There does not seem to be a logical explanation for the fact that the yield stress of only batches C and D was significantly influenced. Batch E had the same partial fill as batch C and the thin shell would theoretically allow even more interaction between the fluid and the bulk of the material. Also, only the cyclic treatments affected the stiffness. A possible cause is the fact that these samples were rinsed 25 times with large quantities of water, however, the exact nature of this chemical reaction should be studied in detail to assess if this is true and to understand what changes take place.

None of these changes were sufficiently large to significantly weaken devices, as long as they are not put under high stress. Reusable tools are usually designed to operate within the lower portion of the elastic region. Therefore, the changes in break stress and strain are more of academic interest than of practical relevance.

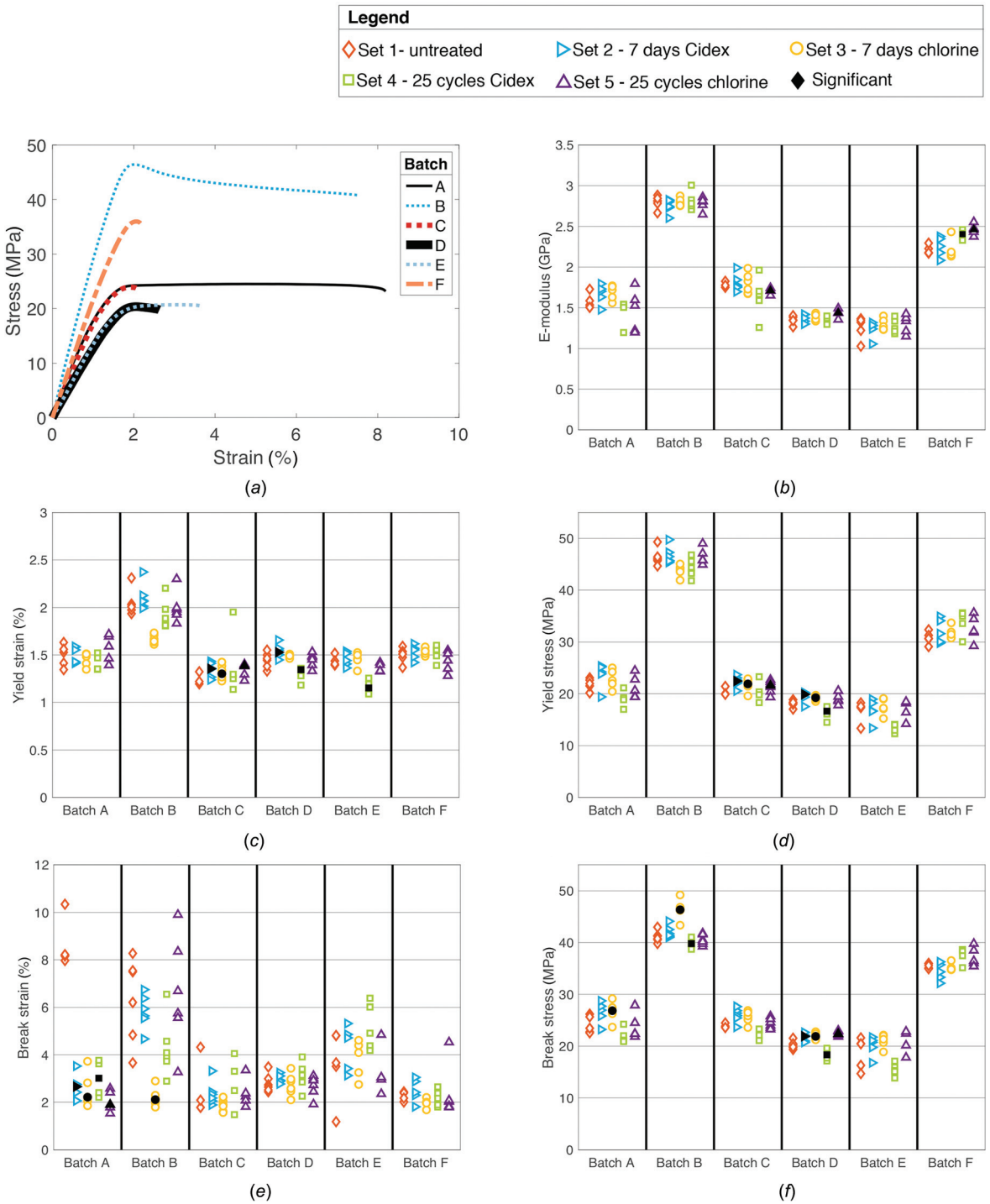

Fig. 3 Graphic overview of results from tensile tests. The legend right above (*b*) is valid for (*b*)–(*e*). A solid filled marker represents the median of a set that is significantly different from set 1. (*a*) Representative stress–strain curve of each batch, (*b*) stiffness measurements for all batches, (*c*) strain at 0.1% offset for batches A, B3, and C–F and strain at yield for batches B1 and B3–B5, (*d*) stress at 0.1% offset for batches A, B3, and C–F and strain at yield for batches B1 and B3–B5, (*e*) strain at break for all batches, and (*f*) stress at break for all batches.

Table 2 Median and (range) of pretreatment sample weight and significant effects of printing and treatment

	A		B		C	D		E		F
Batch	Low quality		High quality		Medium fill	Low fill		Thin shell		Bed
Weight of set 1 (g)	9.1 (8.5–9.2)		10.2 (10.1–10.5)		8.1 (7.9–8.5)	6.6 (6.5–6.8)		7.4 (6.5– 7.6)		9.1 (7.1– 9.1)
Print effect[a]	4		6		1	1		0		4
Treatment effect[b]	Set 2	Set 5	Set 2	Set 3		Set 2	Set 4	Set 4	Set 5	
Median weight increase	1.8%	0.3%	1.1%	0.5%		1.4%	1.8%	8.3%	6.8%	
p-value	0.01	0.04	<0.01	0.01		<0.01	0.01	0.01	0.02	

[a]This row shows the number of set pairs within each batch that differed significantly from each other directly after printing.
[b]The sets that differed significantly in weight before and after treatment are listed.

However, the increased variability of both stiffness and strength post-treatment does have practical consequences for designers.

4.3 Implications for Designing Three-Dimensional Printed Healthcare Devices. The major concern that arose from this study is the absorption of chemical cleaning agent and the possibility to transfer it to human tissue. Depending on the use of the tool, the presence of chemical cleaning agent on the surface may or may not be acceptable. Reducing porosity of the 3D-printed surface seems essential to prevent absorption, which can be obtained with a combination of low printing speed, high printing temperatures, and at least four shell perimeters.

Medical devices are usually designed to operate within the range of elastic deformation and it is common to select materials whose yield stress is three times that of the expected stress during use. Therefore, the changes in yield stress of the magnitude observed in this study are not likely to influence safe use of 3D-printed medical tools. For long continuous as well as short cyclic soaks, cleaning with Cidex OPA and a chlorine solution seems safe from a mechanical point of view. Taking into account the variable nature of 3D printing itself and the increased variability of some of the characteristics post-treatment, it is advisable to use a large safety factor when designing 3D-printed medical tools that will be cleaned. Selecting the appropriate slicer settings is a key in obtaining the appropriate stiffness, strength, and surface porosity.

Medical tools are put into chemical cleaning agents to soak and in order for the disinfectant to be effective on all surfaces, the devices must sink. PLA has a low density and designers must ensure that there is sufficient fill percentage to make sure a tool sinks.

However, before designing a device to be compatible with chemical cleaning, it is important to realize that stiffness and printed resolution are critical to assess the feasibility of 3D-printed medical tools. This has been (partially) done for some designs including umbilical cord clamps, surgical retractors, and stethoscopes, but not for surgical instruments such as forceps [6–8]. Since these issues are device-specific, the usability of each of these 3D-printed tools must be proven in a clinical setting.

4.4 Limitations. This study is limited by the fact that it took place indoors, at room temperature in a nonhumid environment, and therefore, not directly comparable to LMICs [31]. The effect of high temperature on PLA is anecdotally described to weaken the material, and high humidity levels may also cause moisture absorption and weakening of the material. It was not possible to assess to what extent the moisture absorption was a consequence of soaking in the chemical cleaning agent or rinsing in water. Despite identifying the risks related to transfer of the cleaning agent to human tissue, the magnitude of this risk has not been quantified. Also, Ultimakers are relatively expensive 3D printers and not widely available in LMICs, the same goes for the filament. It can be expected that the mechanical properties of the samples with similar slicer settings are comparable between batches, but the absolute values will be different for other printers and filament types. Changes of similar magnitude were observed for both the 25 short and single long treatments. It is possible that additional short cyclic treatments lead to larger material changes, and therefore, an additional number of cycles must be done to investigate this. Also, the gyroid fill is the most isotropic geometric pattern currently available in Cura. Using a more anisotropic fill pattern could cause changes in mechanical properties of different magnitudes than found in this study. Finally, the number of printed samples per set was at least 5 in accordance with the ASTM D638 standard, but the variability that is inherent to 3D printing might be better captured with large numbers of samples.

Most of the samples in this study had a very irregular bottom surface because they were stacked in the 3D printer, whereas most investigations concerning the mechanical properties of 3D-printed materials use samples that are printed directly on the bed. This should be taken into account when designing and when comparing print results to this study. However, 3D-printed samples will always have a rough surface as a consequence of the layered extrusion. Also, curved or slanted surfaces are often part of a design, which may affect the porosity and roughness. Chemical cleaning agents are usually designed to work on smooth surfaces. Rankin et al. [7] showed that glutaraldehyde was effective on a retractor in a single experiment, but the effectiveness of chemical cleaning of ridged 3D-printed PLA samples has not yet been proven in a larger study. This study focused on two disinfectants, but additional work is required to include other commonly used cleaning agents in LMICs such as glutaraldehyde. Without this knowledge, the safe reuse of 3D-printed PLA tools that must be sterile cannot be guaranteed.

5 Conclusions

In this study, it was shown that the median stiffness and strength of 3D-printed PLA samples can be altered up to 13.6% and 12.5%, respectively, due to cleaning with Cidex OPA or a chlorine solution. Safe and reliable mechanical performance of 3D-printed medical tools can be ensured by using a large safety factor to account for the variability in mechanical properties due to 3D printing itself and as a consequence of chemical cleaning. However, soaking in these chemical cleaning agents can lead to absorption of the disinfectant and may possibly cause undesirable transfer to skin or tissue. High-quality 3D-printed surfaces should be created using appropriate printer settings and fill patterns to prevent this from happening. If these conditions are met, 3D-printed medical tools are mechanically fit to clean and reuse. However, additional research is required to establish both the effectiveness of chemical cleaning agents on various 3D-printed surfaces and the risks of human contact with these 3D-printed objects after they have absorbed the cleaning agent.

Acknowledgment

The authors would like to thank Sander Leeflang for his support in preparing the tensile tests and Jan van Frankenhuyzen for his support in preparing the samples.

Funding Data

- TU Delft | Global Initiative (Funder ID: 10.13039/501100001831).

Appendix

Table 3 Median and range of weights in (g) per set and *p*-value of pre- and post-treatment comparison

Batch	Set 1—control	Set 2—Cidex 7 days	Set 3—chlorine 7 days	Set 4—Cidex 25 cycles	Set 5—chlorine 25 cycles
A—low quality					
Pre-treatment	9.1 (8.5–9.2)	9.1 (8.5–9.2)	9.2 (8.4–9.2)	9.2 (8.5–9.3)	9.3 (8.6–9.3)
Post-treatment	—	9.3 (8.5–9.3)	9.2 (8.4–9.3)	9.2 (8.5–9.3)	9.3 (8.9–9.4)
p-value	—	0.01	0.38	0.12	0.04
B—high quality					
Pre-treatment	10.2 (10.1–10.5)	10.2 (10.2–10.3)	10.2 (10.2–10.5)	10.2 (10.2–10.5)	10.3 (10.2–10.6)
Post-treatment	—	10.3 (10.2–10.6)	10.3 (10.2–10.6)	10.2 (10.2–10.5)	10.3 (10.2–10.6)
p-value	—	<0.01	0.01	0.79	0.68
C—medium fill					
Pre-treatment	8.1 (7.9–8.5)	8.2 (7.9–8.5)	8.1 (7.9–8.5)	8.2 (8.1–8.5)	8.1 (7.9–8.2)
Post-treatment	—	8.3 (8.1–8.7)	8.2 (8.0–8.5)	8.3 (8.1–8.5)	8.1 (7.9–8.4)
p-value	—	0.14	0.47	0.38	0.24
D—low fill					
Pre-treatment	6.6 (6.5–6.8)	6.8 (6.5–6.8)	6.6 (6.5–6.7)	6.6 (6.5–6.7)	6.6 (6.6–6.8)
Post-treatment	—	6.8 (6.7–7.0)	6.6 (6.5–6.7)	6.7 (6.5–6.8)	6.7 (6.6–6.9)
p-value	—	<0.01	0.10	0.01	0.10
E—thin shell					
Pre-treatment	7.4 (6.5–7.6)	7.4 (6.4–7.6)	7.5 (6.8–7.6)	7.4 (6.7–7.5)	7.6 (6.7–7.7)
Post-treatment	—	7.7 (6.8–8.3)	7.5 (6.5–7.7)	8.1 (6.8–8.2)	8.1 (6.7–8.3)
p-value	—	0.10	0.38	0.01	0.02
F—bed					
Pre-treatment	9.1 (7.1–9.1)	9.1 (9.1–9.4)	9.1 (9.1–9.5)	9.5 (8.7–9.6)	9.5 (8.7–9.6)
Post-treatment	—	9.2 (9.2–9.5)	9.2 (8.6–9.5)	9.5 (8.7–9.6)	9.5 (8.7–9.6)
p-value	—	0.05	0.08	0.34	0.52

Table 4 Median and (range) for *E*-modulus in GPa

Set	Batch	A Low quality	B High quality	C Medium fill	D Low fill	E Thin shell	F Bed
1	Control	1.5 (1.5–1.7)	2.8 (2.7–2.9)	1.8 (1.8–1.8)	1.3 (1.3–1.4)	1.3 (1.0–1.4)	2.2 (2.2–2.3)
2	Cidex 7 days	1.7 (1.5–1.8)	2.8 (2.6–2.8)	1.8 (1.7–2.0)	1.4 (1.3–1.4)	1.3 (1.1–1.3)	2.3 (2.1–2.4)
3	Chlorine 7 days	1.7 (1.6–1.8)	2.8 (2.8–2.9)	1.8 (1.7–2.0)	1.4 (1.3–1.4)	1.3 (1.2–1.4)	2.2 (2.1–2.4)
4	Cidex 25 cycles	1.5 (1.2–1.5)	2.8 (2.7–3.0)	1.7 (1.3–2.0)	1.4 (1.3–1.4)	1.2 (1.2–1.4)	**2.4 (2.3–2.5)**
5	Chlorine 25 cycles	1.5 (1.2–1.8)	2.8 (2.6–2.9)	**1.7 (1.7–1.7)**	**1.4 (1.4–1.5)**	1.3 (1.1–1.4)	**2.5 (2.4–2.6)**

Batches whose *E*-modulus is significantly different from the untreated batch with the same printer settings are shown in bold.

Table 5 Median and (range) for yield strain at 0.1% offset in %

Set	Batch	A Low quality	B High quality	C Medium fill	D Low fill	E Thin shell	F Bed
1	Control	1.5 (1.3–1.6)	2.0 (1.9–2.3)[a]	1.2 (1.2–1.3)	1.5 (1.3–1.6)	1.4 (1.4–1.5)	1.5 (1.4–1.6)
2	Cidex 7 days	1.6 (1.4–1.6)	2.1 (2.0–2.4)[a]	**1.4 (1.2–1.4)**	**1.5 (1.4–1.7)**	1.4 (1.4–1.5)	1.6 (1.4–1.6)
3	Chlorine 7 days	1.5 (1.3–1.5)	1.7(1.6 – 1.7)[b]	**1.3 (1.2–1.4)**	1.5 (1.5–1.5)	1.5 (1.3–1.5)	1.5 (1.5–1.6)
4	Cidex 25 cycles	1.4 (1.3–1.5)	1.9 (1.8–2.2)[a]	1.3 (1.1–2.0)	**1.3 (1.2–1.4)**	**1.2 (1.1–1.3)**	1.5 (1.4–1.6)
5	Chlorine 25 cycles	1.6 (1.4–1.7)	2.0 (1.8–2.3)[a]	**1.4 (1.2–1.4)**	1.5 (1.3–1.5)	1.4 (1.3–1.4)	1.4 (1.3–1.5)

[a]These values in batch B represent stress at the actual yield point.
[b]Batch B3 no longer had a yield point.
Sets whose stress at 0.1 % offset is significantly different from the untreated set 1 within its batch with the same printer settings are shown in bold.

Table 6 Median and (range) for stress at 0.1% offset in MPa

Set	Batch	A Low quality	B High quality	C Medium fill	D Low fill	E Thin shell	F Bed
1	Control	22.0 (20.1–23.1)	46.0 (44.7–49.0)[a]	20.0 (19.9–21.4)	18.2 (17.0–18.8)	17.4 (13.3–18.2)	30.7 (29.1–32.4)
2	Cidex 7 days	24.2 (19.4–25.4)	46.1 (45.4–0.0)[a]	**22.5 (20.5–23.7)**	**19.9 (17.5–20.2)**	16.7 (13.4–18.9)	31.6 (29.8–34.9)
3	Chlorine 7 days	22.6 (20.4–25.0)	44.0 (41.9–45.1)[b]	**21.9 (19.6–22.9)**	**19.2 (18.5–19.7)**	17.2 (15.2–19.1)	31.5 (30.8–33.7)
4	Cidex 25 cycles	19.0 (17.0–21.1)	43.9 (41.8–0.0)[a]	20.1 (18.3–23.3)	**16.6 (14.5–17.5)**	14.0 (12.3–14.0)	35.0 (30.0–35.7)
5	Chlorine 25 cycles	20.6 (19.4–24.5)	45.8 (44.9–49.0)[a]	**21.6 (19.3–22.7)**	19.1 (17.8–20.6)	17.3 (14.2–18.5)	32.1 (29.2–35.7)

[a]These values in batch B represent strain at the actual yield point.
[b]Batch B3 no longer had a yield point.
Sets whose stress at 0.1 % offset is significantly different from the untreated set 1 within its batch with the same printer settings are shown in bold.

Table 7 Median and (range) elongation at break in %

Set	Batch	A Low quality	B High quality	C Medium fill	D Low fill	E Thin shell	F Bed
1	Control	8.2 (8.0–10.3)	6.8 (3.7–8.3)	2.1 (1.8–4.3)	2.7 (2.4–3.5)	3.7 (1.2–4.8)	2.2 (2.0–2.4)
2	Cidex 7 days	**2.7 (2.1–3.5)**	5.8 (4.7–6.7)	2.3 (1.9–3.3)	2.9 (2.8–3.2)	4.7 (3.1–5.3)	2.4 (1.8–3.0)
3	Chlorine 7 days	**2.2 (1.8–3.7)**	**2.1 (1.8–2.9)**	1.9 (1.6–2.2)	2.7 (2.1–3.4)	4.1 (2.7–4.6)	2.0 (1.7–2.2)
4	Cidex 25 cycles	**3.0 (2.2–3.8)**	4.0 (2.9–6.5)	2.9 (1.5–4.1)	3.2 (2.3–3.9)	4.9 (4.2–6.4)	2.2 (1.8–2.6)
5	Chlorine 25 cycles	**1.9 (1.5–2.6)**	6.2 (3.3–9.9)	2.2 (1.8–3.4)	2.8 (1.9–3.1)	3.0 (2.3–4.8)	2.0 (1.8–4.5)

Sets whose elongation at break is significantly different from the untreated set 1 within its batch are shown in bold.

Table 8 Median and (range) stress or strength at break in MPa

Set	Batch	A Low quality	B High quality	C Medium fill	D Low fill	E Thin shell	F Bed
1	Control	23.5 (22.6–26.2)	41.0 (39.8–43.0)	23.9 (23.6–24.5)	20.0 (19.4–21.5)	20.5 (14.7–21.6)	35.6 (34.9–36.0)
2	Cidex 7 days	27.0 (23.2–28.7)	41.6 (41.0–44.1)	26.1 (23.7–27.7)	**21.9 (20.7–22.7)**	20.8 (16.8–21.8)	34.3 (32.1–36.3)
3	Chlorine 7 days	**26.9 (23.7–29.2)**	**46.3 (43.4–49.2)**	25.8 (23.6–26.9)	**21.9 (21.2–22.8)**	21.3 (18.9–22.2)	34.8 (34.7–36.5)
4	Cidex 25 cycles	21.6 (20.9–24.3)	**39.8 (38.7–41.1)**	22.6 (21.1–23.3)	**18.3 (17.2–19.6)**	15.3 (13.9–17.1)	38.3 (35.1–38.6)
5	Chlorine 25 cycles	22.4 (21.8–27.9)	40.3 (39.3–41.8)	24.3 (23.3–25.8)	**22.4 (21.8–23.0)**	21.3 (17.8–22.8)	36.4 (35.4–39.8)

Sets whose stress at break is significantly different from the untreated set 1 within its batch are shown in bold.

References

[1] IHME, 2014, "Health Service Provision in Kenya: Assessing Facility Capacity, Costs of Care, and Patient Perspectives," Institute for Health Metrics and Evaluation, Seattle, WA.

[2] Oosting, R., Wauben, L., Groen, R., and Dankelman, J., 2019, "Equipment for Essential Surgical Care in 9 Countries Across Africa: Availability, Barriers and Need for Novel Design," Health Technol., **9**(3), pp. 269–275.

[3] Perry, L., and Malkin, R., 2011, "Effectiveness of Medical Equipment Donations to Improve Health Systems: How Much Medical Equipment is Broken in the Developing World?," Med Biol Eng Comput., **49**(7), pp. 719–722.

[4] Malkin, R., and Keane, A., 2010, "Evidence-Based Approach to the Maintenance of Laboratory and Medical Equipment in Resource-Poor Settings," Med & Biol Eng Comput., **48**(7), pp. 721–726.

[5] James, E., and Gilman, D., 2016, "Shrinking the Supply Chain: Hyperlocal Manufacturing and 3D Printing in Humanitarian Response," UN, Den Haag, The Netherlands.

[6] Bhatia, S. K., and Ramadurai, K. W., 2017, *3D Printing and Bio-Based Materials in Global Health*, Springer, Cham, Switzerland.

[7] Rankin, T. M., Giovinco, N. A., Cucher, D. J., Watts, G., Hurwitz, B., and Armstrong, D. G., 2014, "Three-Dimensional Printing Surgical Instruments: Are We There Yet?," J. Surg. Res., **189**(2), pp. 193–197.

[8] Pavlosky, A., Glauche, J., Chambers, S., Al-Alawi, M., Yanev, K., and Loubani, T., 2018, "Validation of an Effective, Low Cost, Free/Open Access 3D-Printed Stethoscope," PLoS One, **13**(3), p. e0193087.

[9] Kats, D., Spicher, L., Savonen, B., and Gershenson, J., 2018, "Paper 3D Printing to Supplement Rural Healthcare Supplies-What Do Healthcare Facilities Want?," IEEE Global Humanitarian Technology Conference (GHTC), San Jose, CA, Oct. 18–21, pp. 1–8.

[10] Ibrahim, A. M., Jose, R. R., Rabie, A. N., Gerstle, T. L., Lee, B. T., and Lin, S. J., 2015, "Three-Dimensional Printing in Developing Countries," Plast. Reconstr. Surg. Global Open, **3**(7), p. e443.

[11] Savonen, B., Mahan, T., Curtis, M., Schreier, J., Gershenson, J., and Pearce, J., 2018, "Development of a Resilient 3-D Printer for Humanitarian Crisis Response," Technologies, **6**(1), p. 30.

[12] Kondor, S., Grant, C. G., Liacouras, P., Schmid, M. J. R., Parsons, L. M., Rastogi, V. K., Smith, L. S., Macy, B., Sabart, B., and Macedonia, C., 2013, "On Demand Additive Manufacturing of a Basic Surgical Kit," ASME J. Med. Devices, **7**(3), p. 030916.

[13] John, A., John, S., and Lambert, C., 2017, "Development and Testing of a Low Cost Videolaryngoscope in a Resource Limited Setting," Ann. Global Health, **1**(83), pp. 4–5.

[14] Meara, J. G., Leather, A. J., Hagander, L., Alkire, B. C., Alonso, N., Ameh, E. A., Bickler, S. W., Conteh, L., Dare, A. J., Davies, J., Derivois Merisier, E., El-Halabi, S., Farmer, P., Gawande, A., Gillies, R., Greenberg, S. L. M., Grimes, C. E., Gruen, R. L., Adan Ismail, E., Buya Kamara, T., Lavy, C., Lundeg, G., Mkandawire, N. C., Raykar, N. P., Riesel, J. N., Rodas, E., Rose, J., Roy, N., Shrime, M. G., Sullivan, R., Verguet, S., Watters, D., Weiser, T. G., Wilson, I. H., Yamey, G., and Yip, W., 2015, "Global Surgery 2030: Evidence and Solutions for Achieving Health, Welfare, and Economic Development," Lancet, **386**(9993), pp. 569–624.

[15] Chao, T. E., Mandigo, M., Opoku-Anane, J., and Maine, R., 2016, "Systematic Review of Laparoscopic Surgery in Low-and Middle-Income Countries: Benefits, Challenges, and Strategies," Surg. Endoscopy, **30**(1), pp. 1–10.

[16] Oosting, R., Dankelman, J., Wauben, L., Madete, J., and Groen, R., 2018, "Roadmap for Design of Surgical Equipment for Safe Surgery Worldwide," IEEE Global Humanitarian Technology Conference (GHTC), San Jose, CA, Oct. 18–21, pp. 1–8.

[17] Sastri, V. R., 2013, *Plastics in Medical Devices: Properties, Requirements, and Applications*, William Andrew, Oxford, UK.

[18] McKeen, L. W., 2014, "Plastics Used in Medical Devices," *Handbook of Polymer Applications in Medicine and Medical Devices*, Elsevier, Oxford, UK, pp. 21–53.

[19] Oosting, R. M., Wauben, L. S., Mwaura, S. W., Madete, J. K., Groen, R. S., and Dankelman, J., 2019, "Barriers to Availability of Surgical Equipment in Kenya," Global Clin. Eng. J., **1**(2), pp. 35–42.
[20] Johnson & Johnson, 2006, "Cidex OPA—Ortho-Phthalaldehyde Solution Instruction," Johnson & Johnson, New Brunswick, NJ.
[21] Yew, G., Yusof, A. M., Ishak, Z. M., and Ishiaku, U., 2005, "Water Absorption and Enzymatic Degradation of Poly (Lactic Acid)/Rice Starch Composites," Polym. Degrad. Stab., **90**(3), pp. 488–500.
[22] Song, Y., Li, Y., Song, W., Yee, K., Lee, K.-Y., and Tagarielli, V., 2017, "Measurements of the Mechanical Response of Unidirectional 3D-Printed PLA," Mater. Des., **123**, pp. 154–164.
[23] Subramaniam, S., Samykano, M., Selvamani, S., Ngui, W., Kadirgama, K., Sudhakar, K., and Idris, M., 2019, "Preliminary Investigations of Polylactic Acid (PLA) Properties," AIP Conf. Proc., **2059**, p. 020038.
[24] Alafaghani, A., Qattawi, A., Alrawi, B., and Guzman, A., 2017, "Experimental Optimization of Fused Deposition Modelling Processing Parameters: A Design-for-Manufacturing Approach," Procedia Manuf., **10**, pp. 791–803.
[25] Yang, L., Li, S., Li, Y., Yang, M., and Yuan, Q., 2019, "Experimental Investigations for Optimizing the Extrusion Parameters on FDM PLA Printed Parts," J. Mater. Eng. Perform., **28**(1), pp. 169–182.
[26] Pei, E., Lanzotti, A., Grasso, M., Staiano, G., and Martorelli, M., 2015, "The Impact of Process Parameters on Mechanical Properties of Parts Fabricated in PLA With an Open-Source 3-D Printer," Rapid Prototyping J., **21**(5), pp. 604–617.
[27] Mohamed, O. A., Masood, S. H., Bhowmik, J. L., Nikzad, M., and Azadmanjiri, J., 2016, "Effect of Process Parameters on Dynamic Mechanical Performance of FDM PC/ABS Printed Parts Through Design of Experiment," J. Mater. Eng. Perform., **25**(7), pp. 2922–2935.
[28] ASTM, 2015, "Standard Test Method for Tensile Properties of Plastics," ASTM International, West Conshohocken, PA, Standard No. ASTM D638-14.
[29] World Health Organization and Pan American Health, 2016, "Decontamination and Reprocessing of Medical Devices for Health-Care Facilities," World Health Organization and Pan American Health Organization, Geneva, Switzerland.
[30] Akhoundi, B., and Behravesh, A., 2019, "Effect of Filling Pattern on the Tensile and Flexural Mechanical Properties of FDM 3D Printed Products," Exp. Mech., pp. 1–15.
[31] Neighbour, R., and Eltringham, R., 2012, "The Design of Medical Equipment for Low Income Countries: Dual Standards or Common Sense," 7th International Conference on Appropriate Healthcare Technologies for Developing Countries, IEEE, London, Sept. 18–19.